ANL/XFD/CP--89431 CONF-960848--17

CRYSTAL DIFFRACTION LENS TELESCOPE FOR FOCUSING NUCLEAR GAMMA RAYS*

Robert K. Smither, Patricia B. Fernandez, Timothy Graber
Experimental Facilities Division
Advanced Photon Source, Argonne National Laboratory
Argonne, IL 60439, USA

Peter von Ballmoos, Juan Naya, Francis Albernhe, G. Vedrenne
Centre d'Etude Spatiale des Rayonnements,
9, du Colonel-Roche, 31029 Toulouse, FRANCE

Mohamed Faiz
Physics Department, KFUPM
Dhahran 31261, SAUDI ARABIA

August 1996

INVITED TALK presented at the SPIE 1996 International Symposium on Optical Science, Engineering, and Instrumentation, Session on "Gamma Ray and Cosmic Ray Detectors, Techniques and Missions," Denver, CO, 4-9 August 1996; to be published in the Proceedings.

*This work is supported by the U.S. Department of Energy, Basic Energy Sciences-Materials Sciences, under contract #W-31-109-ENG-38.

Crystal diffraction lens telescope for focusing nuclear gamma rays

Robert K. Smither, Patricia B. Fernandez, Timothy Graber

Advanced Photon Source, Argonne National Laboratory,
9700 S. Cass Avenue, Argonne, IL 60439 USA

Peter von Ballmoos, Juan Naya, Francis Albernhe, G. Vedrenne

Centre d Etude Spatiale des Rayonnements,
9, du Colonel-Roche, 31029 Toulouse, FRANCE

Mohamed Faiz
Physics Department, KFUPM
Dhahran 31261, SAUDI ARABIA

ABSTRACT

A crystal diffraction lens was construct at Argonne National Laboratory for use as a telescope to focus nuclear gamma rays. It consisted of 600 single crystals of germanium arranged in 8 concentric rings. The mounted angle of each crystal was adjusted to intercept and diffract the incoming gamma rays with an accuracy of a few arc sec. The performance of the lens was tested in two ways. In one case, the gamma rays were focused on a single medium size germanium detector. In the second case, the gamma rays were focused on the central germanium detector of a 3x3 matrix of small germanium detectors. The efficiency, image concentration and image quality, and shape were measured. The tests performed with the 3x3 matrix detector system were particularly interesting. The wanted radiation was concentrated in the central detector. The 8 other detectors were used to detect the Compton scattered radiation, and their energy was summed with coincident events in the central detector. This resulted in a detector with the efficiency of a large detector (all 9 elements) and the background of a small detector (only the central element). The use of the 3x3 detector matrix makes it possible to tell if the source is off axis and, if so, to tell in which direction. The crystal lens acts very much like a simple convex lens for visible light. Thus if the source off to the left then the image will focus off to the right illuminating the detector on the right side: telling one in which direction to point the telescope. Possible applications of this type of crystal lens to balloon and satellite experiments will be discussed.

Keywords: crystal lens, gamma ray, diffraction, matrix detector, imaging

1. INTRODUCTION

A large crystal-diffraction telescope was built at Argonne National Laboratory for focusing energetic nuclear gamma rays that are emitted from distant sources. The lens was originally constructed as part of the DOE program for Arms Control and Nonproliferation. The objective was to locate fissile material at distances of 50 to 300 m and/or in well-shielded locations. There was a need to precisely locate the material and determine its shape, as well as what kind and how much of each material was present. It was recognized early in its development that there were astrophysical applications for the crystal-lens telescope as well.[1-6] A collaboration was developed in 1992 between Argonne National Laboratory and the CESR laboratory at the University of Toulouse, Toulouse, France, to explore the application of this type of lens for astrophysics experiments. A number of publication have resulted from this collaboration for both balloon-flight experiments and satellite-carried experiments.[7-11] The construction of the full lens was completed in 1995. Considerable testing of the lens has occurred since with gamma-ray energies from 303 keV to 661.65 keV using both a large single-germanium gamma-ray detector and a 3x3 matrix of 9

germanium detectors. These tests have verified the theoretically predicted response function of the lens for sources both on and off axis and suggest possible improvements in the design of the lens for future experiments. The next step in the development of the lens is to automate the focusing of the lens so that one can use a computer to focus the lens at a new distance and/or change the energy of the gamma ray being focused. Preliminary experiments with adjusters and position sensors indicate that this can be done with commercially available components.

2. DESCRIPTION OF THE CRYSTAL LENS

The crystal lens consists of 600 single crystals of germanium mounted in 8 concentric rings. Each ring uses a different set of crystalline planes to diffract the gamma rays to a common focal spot behind the lens. The radius of each ring is chosen so that each ring focuses the gamma rays at a common focal distance.

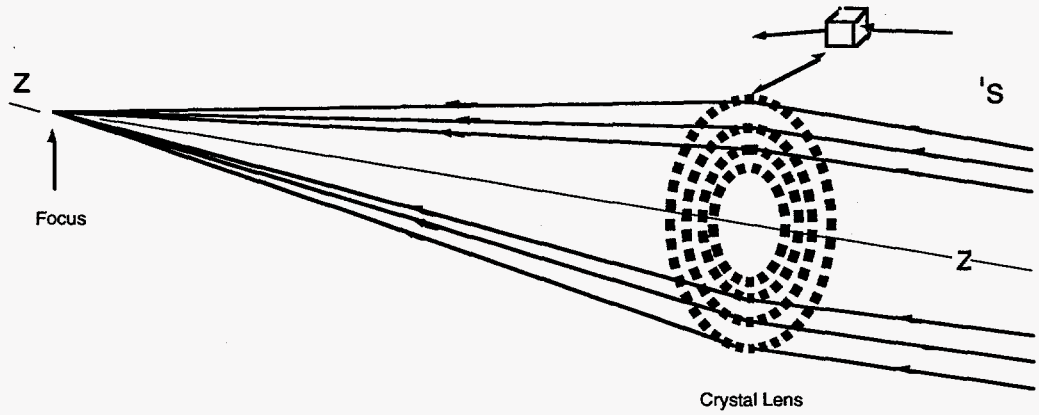

Figure 1 A schematic view of the crystal lens is shown focusing gamma rays from a distant source.

Figure 1 shows a schematic view of the lens focusing gamma rays from a distance source. Figure 2 shows a front view of the lens. The crystalline planes used in the diffraction process, starting with the smallest ring are [111], [220], [311], [400], [331], [422], [333], and [440], respectively. Most of the crystals are cubes 0.93 cm on a side. The crystals in the [331] and [333] rings are narrower in the radial direction (0.83 cm) so that they will fit into a smaller radial space and deeper (1.50 cm) to make up for their weaker diffraction efficiency. The lens frame is made from a stainless steel plate 1.5 cm thick. Figure 3 shows the cross section of the lens with the crystals mounted in each ring on thin aluminum plates. These plates are flexed to adjust the incident angle of the gamma rays on the crystalline planes. The deflection is accomplished by compressing a spring against the plate near its free end. Figure 4 shows this arrangement in detail. By choosing a soft spring that flexes by a distance one hundred times greater than the amount of flex in the aluminum plate for the same force, one can increase the sensitivity of the adjustment by a factor of 100. Thus, the adjusting system behaves as if the lever arm were 150 cm long rather than the actual 1.5 cm. This system allows one to adjust the diffraction angle of the individual crystals with an accuracy of a few arc seconds. The lens frame is mounted in a manner that allows one to rotate it around 3 independent perpendicular axes (x, y, and z). It is also mounted on rails so that its position toward and away from the source can be varied and so that it can be displaced perpendicular to the line from the lens to the source.

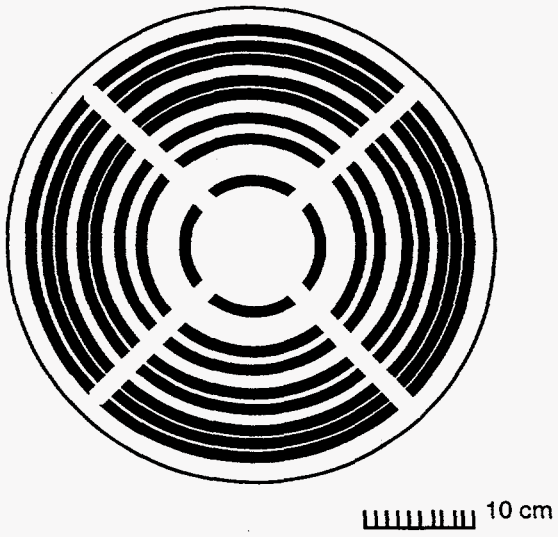

Figure 2 A front view of the Argonne crystal lens.

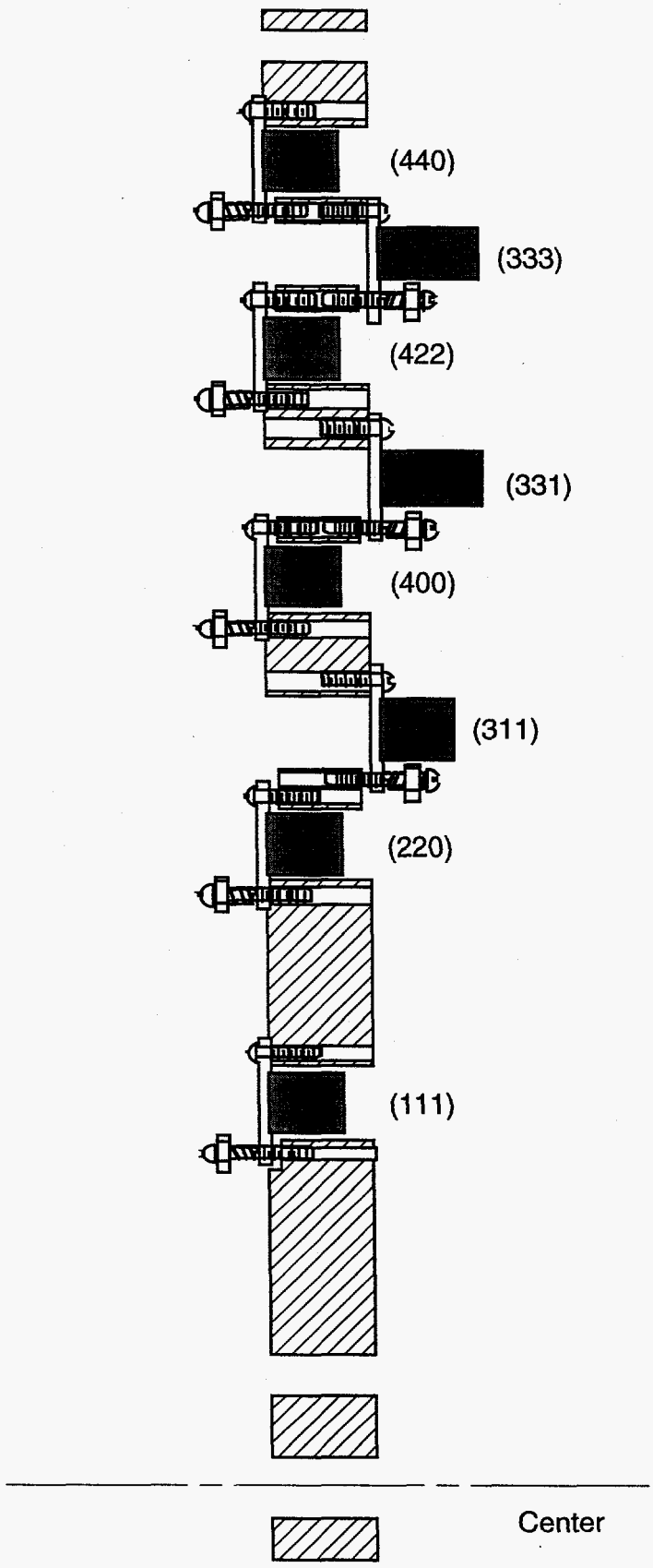

Figure 3 A cross section of the crystal lens frame. The individual crystals are mounted on aluminum plates that are fastened to the lens frame.

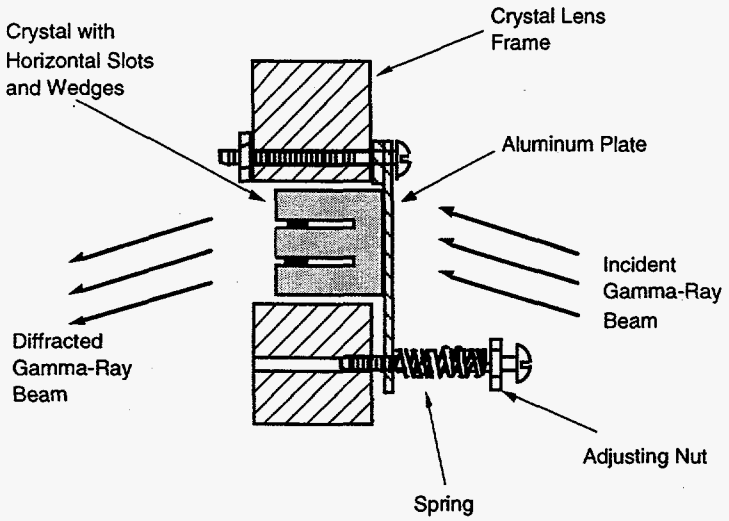

Figure 4 The tuning arrangement for a single crystal consists of a soft spring that flexes by a distance one hundred times greater than the distance the aluminum plate supporting the crystal would flex for the same force. This increases the sensivity of the adjustment by a factor of 100.

3. CRYSTAL LENS THEORY AND FOCUSING PARAMETERS

Equation 1 gives the basic relation that governs crystal diffraction of gamma rays:

$$\lambda = 2d_{hkl} \sin \theta , \tag{1}$$

where λ is the wavelength of the gamma ray, d is the crystalline plane spacing, hkl are the Miller indices that identify the crystalline plane, and θ is the diffraction angle. The focal length of the lens, the distance behind the lens where gamma rays will focus for a source located a long distance away is given by equation 2:

$$\text{Focal length} = \text{R(crystal ring radius)} / \tan 2\theta . \tag{2}$$

Thus the focal length is dependent on the ring radius, the crystalline plane spacing, and the wavelength of the gamma ray. To the first approximation, the focal length is equal to a constant times the energy of the gamma ray. The approximate focal length for the Argonne lens is given by,

$$\text{Focal length (m)} = 1.65 \times 10^{-2} \times E\gamma\,(\text{keV}) . \tag{3}$$

For a source located at a finite distance from the crystal lens, equations 4 and 5 must be satisfied along with equation 1.

$$L_S = R / \tan (\theta - \phi) \tag{4}$$

$$L_D = R / \tan (\theta + \phi) , \tag{5}$$

where L_S is the distance from the source to the lens, L_D is the distance from the lens to the detector and ϕ is the offset angle of the crystalline planes from the symmetric case that is needed to satisfy the Bragg condition given in equation 1.

The small angle approximation gives:

$$1 / FL \text{ (focal length)} = 1 / L_S + 1 / L_D , \quad (6)$$

which corresponds to the simple lens formula for a convex lens with visible light. Thus, it is relatively simple to calculate where the source and detector should be placed if one remembers that the focal length is a function of the gamma-ray energy as given in equation 3.

The focusing of the lens was tested at 7 gamma-ray energies between 661.65 keV and 302.83 keV. A list of these gamma rays with their respective sources, focal lengths, distance from source to lens, and distance from lens to detector appears in table I.

Table I. Gamma-ray sources tested with ANL crystal lens.

Energy (keV)	Source	Focal Length (meters)	Source-Lens (meters)	Lens-Detector (meters)
661.65	^{137}Cs	10.92	24.75	19.54
511.00	^{22}Na	8.43	19.11	15.09
413.7	^{239}Pu	6.83	15.47	12.22
383.71	^{133}Ba	6.33	14.35	11.33
375.2	^{239}Pu	6.19	14.03	11.08
355.94	^{133}Ba	5.87	13.31	10.51
302.83	^{133}Ba	5.00	11.33	9.70

These tests were made without changing the tune (adjusting the orientation of the crystals) of the lens. This is possible by using equations 1-6, because the diffraction angles are small and the value for the tangent of the angle is equal to the value of the sine of the angle to one part in 6600 for the worse case (the outer ring, lowest energy). Thus sinθ changes proportionally as one changes the distance from the source to the lens. This approach does not work for astrophysics sources because one can not change the source to lens distance by any significant amount. For astrophysics sources one must retune the lens to the new energy.

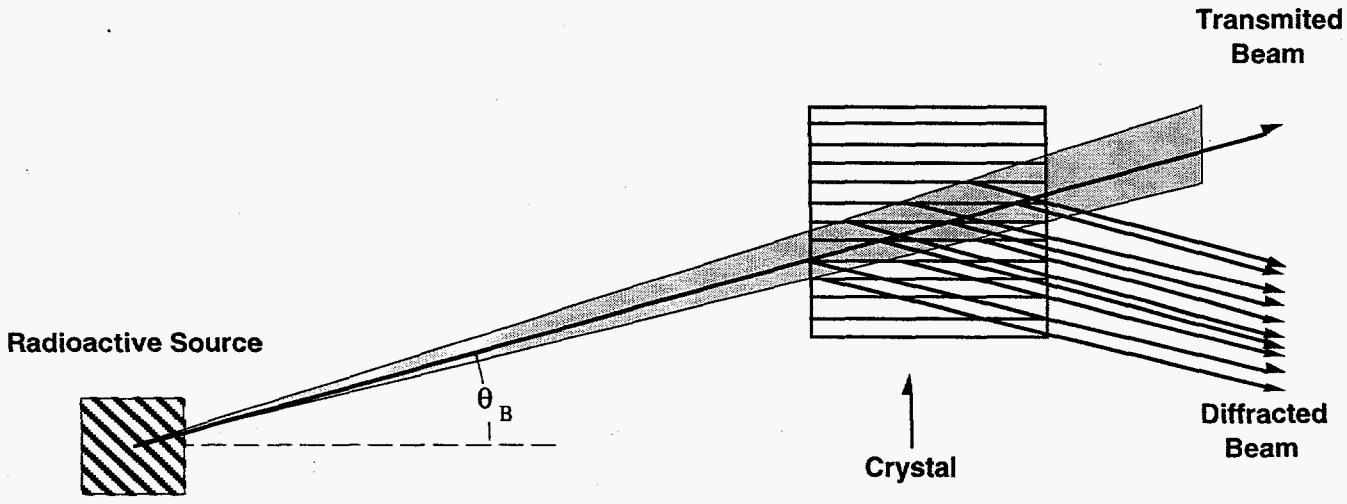

Figure 5 The gamma rays emitted by a point source will only be diffracted by a thin slice of the crystal as shown schematically in the figure. To enhance its diffraction efficiency, each crystal was slotted and wedged. See text.

4. FOCUSING GAMMA RAY PERFORMANCE TESTS

The initial tests for focusing gamma rays were performed with a ^{137}Cs radioactive source of 661.65 keV at 24.75 m from the source. This source is 3 mm in diameter and subtends an angle of 25 arc sec as viewed from the lens. Six of the 8 rings have crystals that are 0.93 cm high and subtend an angle of 77 arc sec as seen from the source. The mosaic structure width of the germanium crystals was measured and found to be in the range between 1 and 2 arc sec. (FWHM). This is much narrower than the subtended angles mentioned above for the crystals and the source and results in a reduction in the volume of the crystal that can contribute to the diffraction at one time. This limitation is illustrated in figure 5. Thus gamma rays emitted from a point on the source will only be diffracted by a thin slice of the crystal. The thickness of this slice will be 2 arc sec divided by 77 arc sec times the radial height of the crystal (9.3 mm) = 0.24 mm or 2.6 percent of the crystal. In order to increase the diffraction efficiency of the crystals, two slots were cut into the back of the crystal to about 2 mm from the front of the crystal and plastic wedges that bent the crystal were inserted in these slots so that the crystalline planes in adjacent sections made an angle of 30 arc sec with one and the other. These cuts and wedges are shown in figure 4. This wedging allowed all three sections of the crystal to contribute to the diffraction process at the same time. With this arrangement, 7.8 percent of the crystal contributed to the intensity of the diffracted beam. Considerable improvement in the diffraction efficiency of the lens will result if one uses crystals with a larger mosaic structure. The best results will be obtained by using crystals with mosaic structure widths that match the angular size of the crystals as seen from the source and/or the angular size of the source as seen from the lens. The combination of the angular width of the source and the angular width of the three segments of the diffraction crystals result in a rocking curve (plot of the intensity of the diffraction line versus the diffraction angle) for the individual crystals of 35 arc sec. Theory predicts that the rocking curve for the full lens made up of rings of crystals will be 1.64 times the rocking curve for the individual crystals: 1.64 times 35 arc sec = 57.4 arc sec. The actual measured rocking curve for the lens when focusing the 661.65 keV line from ^{137}Cs was 60 arc sec. The difference being attributed to the imperfect tuning of the lens; thus the lens was tuned quite well. Figure 6 shows the rocking curve for the lens when focusing the 661.65 keV line. The long

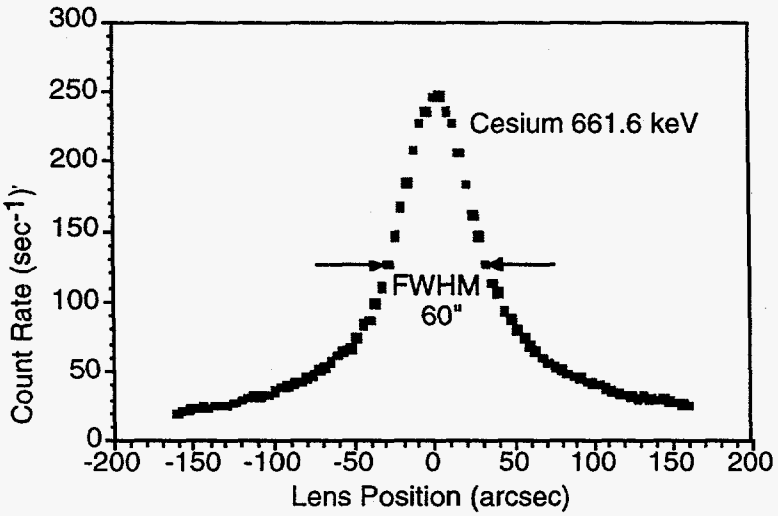

Figure 6 A vertical scan over a 24 arc sec diameter source of 661.65 keV gamma rays from the decay of ^{137}Cs is shown. The wide wings are a real part of the response function of the lens and are related to the circular symmetry of the lens. The background in this experiment was 0.05 counts per sec in the energy window set to detect the full energy peak.

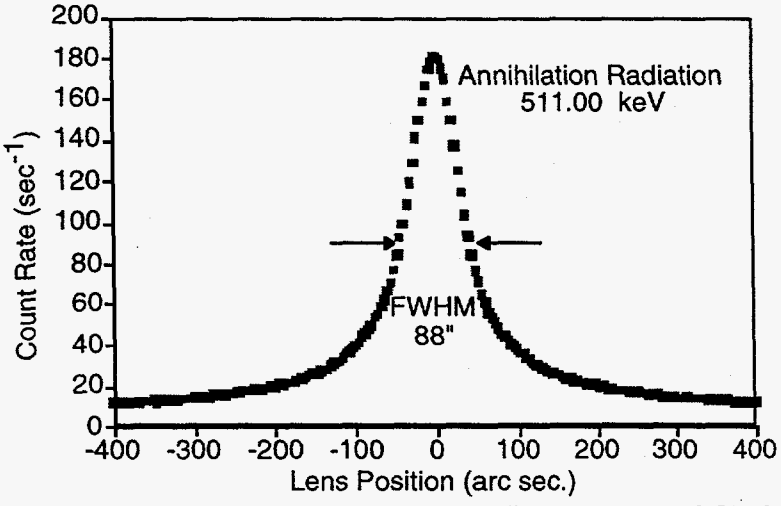

Figure 7 A vertical scan over a 45 arc sec diameter source of 511.0 keV gamma rays from the decay of ^{22}Na is shown. The FWHM of the curve (88 arc sec) is larger than the FWHM observed for the 661.65 keV line because the angular size of the source as seen from the lens is larger than for the Cs source due to the shorter distance from source to lens and the larger size of the source, and due to the mismatch in the wedging of the crystal and this new source-to-lens distance.

wings on the rocking curve are real parts of the curve. The background in these tests was less than 0.5 counts per sec. Figure 7 shows the rocking curve for the 511 keV line from the ^{22}Na source. This rocking curve is wider (88 arc sec). The difference is partly due to the fact that the crystals were wedged properly for the distance to the 661.65 keV line source at 24.75 m from the lens, but improperly for the 511 keV source that was located at 19.11 m from the lens and partly due to the fact that at this closer distance the angle subtended by the crystal as seen from the source and the angle subtended by the source as seen from the lens is now larger.

For sources a long distance away, the effect of the size of the crystal disappears and only the angular size of the source must be taken into account in predicting the efficiency of the lens. The diffraction efficiency of lens is defined as the fraction of the gamma rays incident on the surface of the crystals that are focused on the detector. This efficiency includes the effects of both the diffraction efficiency of the crystalline planes and the absorption of the gamma rays as they pass through the crystal but not the efficiency of the detector.

For a single crystal or for a ring of crystals using the same crystal diffraction planes and with a uniform mosaic spread in its diffraction planes, the diffraction efficiency for Laue diffraction (the transmission case) follows the relationship given in equation 7.

$$I / Io = 1/2 [1 - \exp(-\alpha x)] [\exp (-\mu x)] , \quad (7)$$

where I is the intensity of gamma rays focused on the detector; Io is the intensity of gamma rays incident on the surface of the crystal or crystals; α is the coefficient of crystal diffraction per unit length of crystal material; x is the length of the crystalline material; and μ is the coefficient of atomic absorption of the gamma ray in the crystal. The coefficient α is the effective cross section for diffraction per unit length. The value of α depends on the wavelength of the gamma ray, the crystal material, the diffraction planes used, and the width of the mosaic structure in the crystal. Once one has established the value of α experimentally, at a few energies, one can use equation 7 to predict values for other energies. The diffraction efficiency for the full lens will tend to follow equation 7 as well when one uses a weighted average of the αx values for the individual crystals. For a mosaic crystal, the value of α varies as the square of the wavelength and inversely with the width of the mosaic structure. The crystals used in this lens have a relatively small mosaic spread (1 to 2 arc sec) and are strongly distorted by the wedging, which is proper only for a distance from source to lens of 24.75 m, so efficiency values at other distance are quite difficult to calculate. In the first set of experiments, this distance from source to lens was varied strongly for each gamma-ray energy and had a larger effect on the efficiency than the dependence of α on the square of the wavelength. Thus the efficiency decreases for lower energies and longer wave lengths, rather than increasing. Table II gives the measured efficiencies for the 7 tested gamma rays listed in table I when the distance from source to lens was the value listed in table I.

Table II. Crystal lens efficiency for gamma-ray sources for the case in which the source-to-lens distance varied. The measured values were corrected for air absorption and detector efficiency.

Energy (keV)	Source	Lens Efficiency (percent)	Source-Lens (meters)	Lens-Detector (meters)
661.65	^{137}Cs	5.6	24.75	19.54
511.00	^{22}Na	4.5	19.11	15.09
383.71	^{133}Ba	4.0	14.35	11.33
355.94	^{133}Ba	3.8	13.31	10.51
302.83	^{133}Ba	3.3	11.33	9.70

When the source-to-lens distance was standardized at 24.75 m, the efficiency of the lens at the lower energies did increase with longer wavelengths and followed equation 7 quite well at the lower energies tested. Table III gives the lens efficiencies for the case in which the distance from source to lens is fixed at 24.75 m.

Table III. Crystal lens efficiency for gamma-ray sources for the case in which the source-to-lens distance was fixed at 24.75 m. The measured values were corrected for air absorption and detector efficiency.

Energy (keV)	Source	Lens Efficiency (percent)	Source-Lens (meters)	Lens-Detector (meters)
661.65	^{137}Cs	5.6	24.75	19.54
511.00	^{22}Na	7.7	24.75	12.78
383.71	^{133}Ba	11.8	24.75	8.51
355.94	^{133}Ba	12.9	24.75	7.70
302.83	^{133}Ba	15.3	24.75	6.27

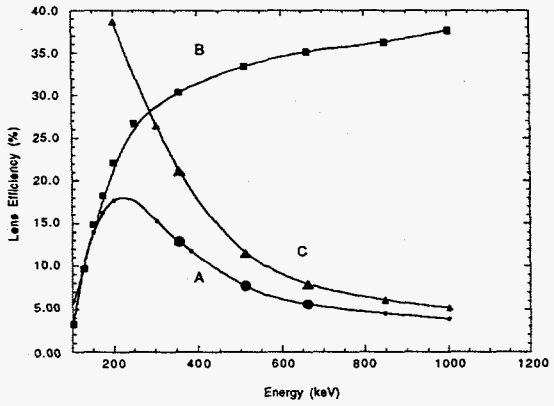

Figure 8 Efficiency values for the case in which the distance from source to lens is fixed at 24.75 m are plotted against gamma-ray energy. The experimentally measured points are shown as large filled circles (curve A). The calculated points are shown as small circles. Also plotted are the values for maximum efficiency at a given gamma-ray energy (curve B, squares). Curve C shows the diffraction efficiency as a function of energy without the effect of gamma-ray absorption in the crystal.

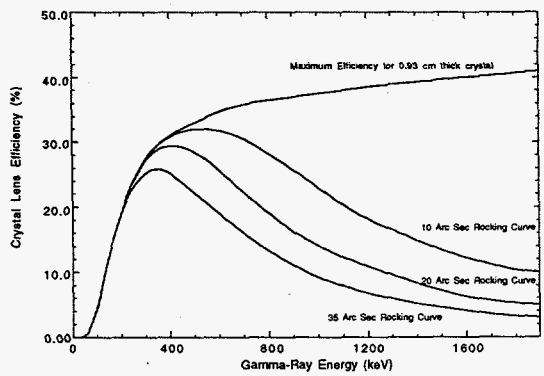

Figure 9 The lens efficiency as a function of energy is shown for three values of mosaic structure width. The maximum efficiency for a lens with 0.93 cm thick crystals is also shown

These efficiency values for the case in which the distance from source to lens is fixed at 24.75 m are plotted against gamma-ray energy in figure 8. The experimentally measured points are shown as large filled circles (curve A). The calculated points are shown as small circles. Also plotted in figure 8 is the curve B, shown as squares, for the values of the maximum efficiency possible for that energy, the case when the cross section for diffraction is very large compared to the cross section for absorption,

$$\text{Max. Efficiency} = 1/2\,[\exp(-\mu x)], \qquad (8)$$

{PAG
E }

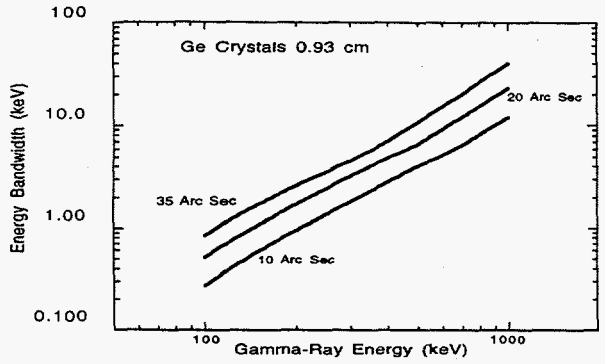

Figure 10 The crystal lens bandwidth (in keV) as a function of gamma-ray energy is shown for the three values of mosaic structure width given in figure 9.

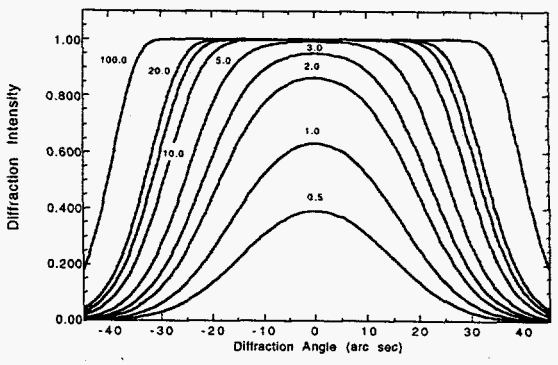

Figure 11 Rocking curves are plotted for crystals with different degrees of saturation.

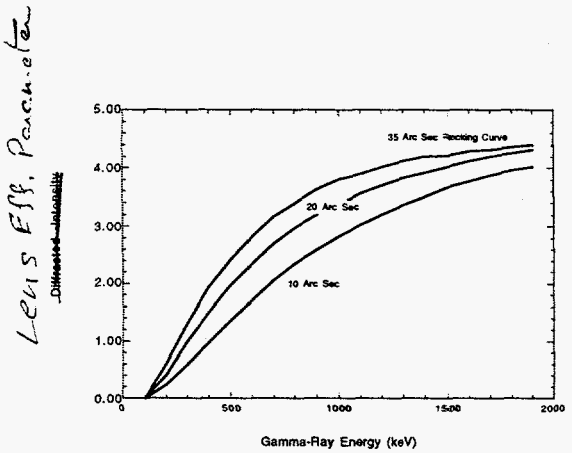

Figure 12 A set of plots of the Lens Efficiency Parameter verses gamma ray energy, for crystals with different mosaic structure widths for the Argonne lens, when looking at a continuum source.

and curve C, the values for crystalline diffraction efficiency only, without the effect of the absorption of the gamma ray in the crystal, shown as triangles.

$$\text{Cry. Diff. Eff.} = 1/2\,[\,1 - \exp(-\alpha x)\,] \qquad (9)$$

The actual distortion of the crystalline planes in these wedged crystals was calculated, and, based on these calculations, one estimates that these crystals would be four times more efficient, that is, α would be 4 times larger than the effective values obtained from the measurement of the wedged crystals. Figure 9 shows plots of the lens efficiency assuming three different values for the mosaic structure width (FWHM) for a monochromatic point source a long distance away. At the low energy end of the graph, all three curves saturate at the maximum value set by one half of the transmitted gamma ray beam value set by equation 8. At the high energy end of the plot, the curves for the lower value of the mosaic structure width are better. There is a price to pay for this improved efficiency, in that a narrower mosaic structure width also means that the energy bandwidth for the gamma rays diffracted at any one time is narrower. Also, the field of view of the lens is narrower. If the energy of the gamma-ray line is broadened due to things such as Doppler-shift broadening, one could lose some of the intensity. Figure 10 shows the bandwidth in keV as a function of the gamma-ray energy for three values of the width of the mosaic structure. These are the same mosaic widths as those used for the curves in figure 9. Normally these plots would be straight lines on a log-log plot, but in this case, the diffraction efficiency saturates at the low energy end of the plot, increasing the bandwidth of the diffracted energy. Figure 11 shows the response function or rocking curve (diffraction intensity as a function of diffraction angle) for crystals with different degrees of saturation. The curves are labeled with the corresponding value of αx as used in the equations cited above. The full width at half maximum for the unsaturated response function is 35 arc sec in this example. The shape of this curve determines the energy bandwidth that the crystal will diffract when the diffraction angle of the crystal is held constant. When one views a continuum energy source rather than a monochromatic source, the intensity of the diffracted beam will depend on this energy bandwidth. Thus the calculation of the focused gamma ray flux will require one to integrate the flux diffracted by this response function. For a mosaic crystal where the spread in the mosaic structure is large compared to the Darwin width, the width of the response function will remain constant in its angular width

and not change width energy. $\Delta E/E$ is approximately equal to $\Delta\theta/\theta$. The corresponding energy bandpass will therefore increase with energy. This comes about because the diffraction angle θ decreases with increasing energy while $\Delta\theta$ remains constant. In order to calculate the focused flux from a continuum source, one must combine these bandwidth effects with the diffraction efficiency. To facilitate the calculation of the flux of the focused beam, one can calculate a "Lens Efficiency Parameter" that, when multiplied by the area of the lens and the gamma ray flux / cm2 / sec / keV, will give the focused flux per sec. Figure 12 shows the "Lens Efficiency Parameter," when the lens is looking at a continuum source, for the same lens, who's crystal lens efficiency for a monochromatic source, is plotted in figure 9. Again, three curves are shown for 3 different mosaic structure widths. In the continuum case, figure 12, the wider mosaic structure results in the stronger diffracted beam. The relative differences become smaller at the higher energies because the higher efficiency for monochromatic radiation for crystals with narrow rocking curves partly compensates for the larger bandpass associated with crystals with wider mosaic structure spreads. The intensity of the diffracted beam is calculated by multiplying the photons per sec per keV per cm^2 by the area of the crystals in the lens, and then by the vertical scale reading for the desired mosaic structure width and desired energy in figure 12. Thus, if the number of photons per sec per keV per cm^2 is 10^{-6}, the area of crystal surface is 600 cm^2, the mosaic structure width is 35 arc sec, and the energy of the gamma ray is 847 keV, then the diffracted flux of gamma rays is equal to 2.1×10^{-3} photons per sec.

5. SINGLE AND MULTIPLE MATRIX Ge DETECTORS

One of the most attractive features of the lens is that it focuses all of the wanted radiation onto a small focal spot. This allows one to select a detector that is the right size for detecting the full energy of the gamma ray and decouples the detector size from the collection area of the crystal lens. Thus one can keep the background constant while increasing the signal by increasing the size of the lens. When focusing the gamma rays onto a small spot on a single germanium detector of optimum size, the efficiency for detecting the full energy of the gamma ray is enhanced for the more energetic gamma rays. This is because the first interaction occurs near the center of the detector, and one has a better chance of stopping the Compton-scattered gamma rays in the rest of the detector than if the first interaction occurred near the edge. The single germanium detector used in most of the lens experiments was 6 cm in diameter and 6 cm deep. The 1 cm outer ring of the detector, which has 56 percent of the area of the face of the detector, was measured to have about 50 percent less efficiency in detecting the full energy of 661.65 keV gamma rays than areas inside the 2 cm radius. This effect is caused by the higher rate of escape of the Compton-scattered gamma rays from this outer ring. The net effect of this concentration is to increase the efficiency of the detector for the full energy peak by 30 percent.

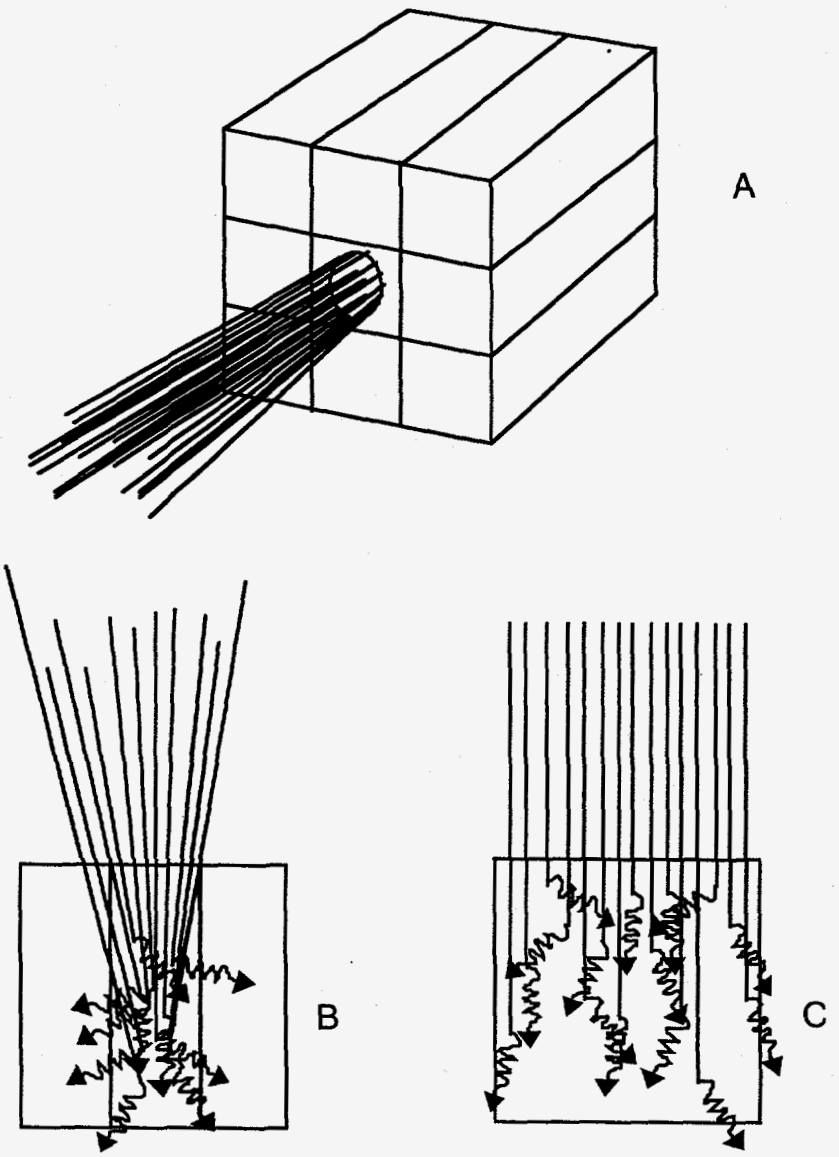

Figure 13 Schematic representations of (a) the CESR 3 x 3 matrix detector with a gamma ray beam focused on the center element, (b) a cross section of the 3 x 3 matrix detector showing the interaction of the focused beam in the detector, (c) the cross section of a normal detector, showing the interaction of a nonfocused beam.

The astrophysics group at CESR in Toulouse France have developed a multi-element germanium detector that is a 3 x 3 matrix of germanium gamma-ray detectors. Each element is 1.5 cm by 1.5 cm on its face and 4 cm deep.[9,11] This new type of detector turns out to be an ideal detector for the crystal lens in that it allows one to take advantage of the focusing properties of the lens to concentrate the wanted radiation on the center element in the 3 x 3 matrix. This results in the ideal situation where one has only to compete with the background in the center element while the other 8 germanium detectors are used to detect the Compton-scattered gamma rays in coincidence with the first interaction in the center detector. (This gives a detector background similar to one from a detector the size of the center element, but an efficiency for detecting the full energy peak similar to a detector the size of the full matrix.) The CESR detector was brought to Argonne and tested in combination with the Argonne crystal lens. The combination worked quite well, and the background was reduced by a factor of 8 over the background in the full matrix detector. This effect is illustrated in figure 13.

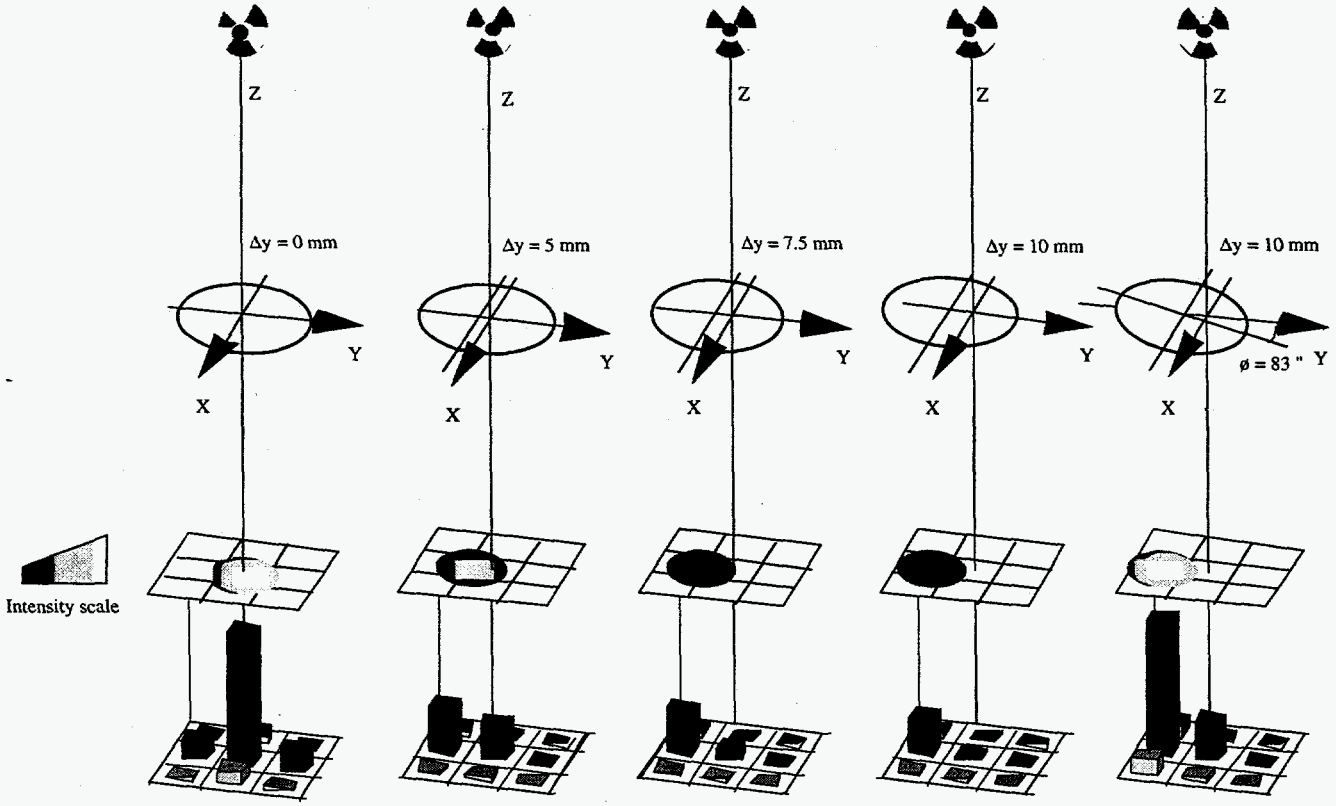

Figure 14 The telescope response for focusing off-axis sources. The first (left) drawing shows the system performance when the source, lens , and array are perfectly aligned. The following three drawings show the evolution of the focal spot position as well as the diffraction efficiency when the lens is displaced along the y axis. Finally, the last (right) drawing shows a measurement when the lens is tilted such that it is aligned with the source.

Another important feature of this combination of crystal lens and matrix detector is that one can sense when the source is off axis and, just as important, the direction in which it is off axis. This is illustrated in the experimental results shown in figure 14. As the source moves off axis to the right, the image of the source focused on the detector moves off the center detector and onto the detector on its left. If the lens is now rotated to point at the off-axis source without moving the detector, then the off center count rate is enhanced, confirming the direction that the source is off axis and giving a measure of how much the source is off axis. This will be of considerable value when one is searching for a small source. This off-axis response suggests that one could extend this concept and use a larger matrix detector, a 4 x 4 or 5 x 5 or 4 x 6 matrix of detectors, to increase the field of view without losing the signal-to-background advantage discussed above. This approach could have considerable advantage if one wanted to scan a small angular area or track a source as the space craft changes orientation. One could just move the lens and not the detector or the space craft to follow the motion of the source or complete a scan in angle. This would be much easier and require much less energy than moving the full telescope or the satellite.

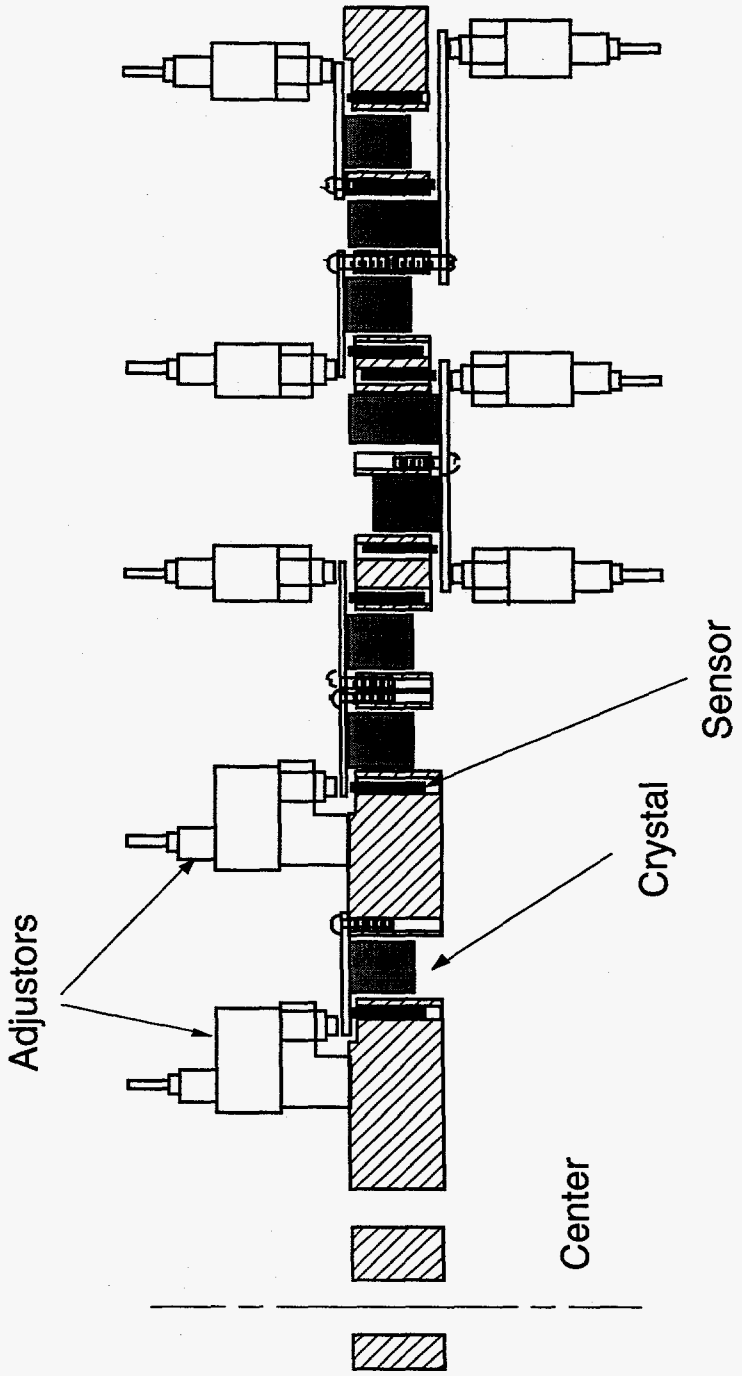

Figure 15 A cross section of the lens with the position sensors and the adjusters in place.

6. COMPUTER CONTROLLED TUNABLE LENS

One feature that needs to be developed before one can seriously consider a satellite flight or a mobile ground application is a method to automatically retune the lens to a new energy (and/or a new distance for ground applications) through an appropriate computer control system. A new lens is under construction that will allow this to be accomplished. The first of 8 rings has been mounted. The diffraction angle of the individual crystals is adjusted with a small picomotor made by New Focus. The actual position and thus the diffraction angle is monitored with a Kaman noncontact position sensor. Experiments with this system have just begun, but the initial results are very encouraging. The main challenge is to obtain good temperature stability. It should be able to change energies in 5 to 10 minutes under computer control after the system is calibrated. This compares to the one to two month effort required if it is done by hand with the present system. Figure 15 shows a schematic view of how the cross section of the lens would look with the adjusters and sensors in place.

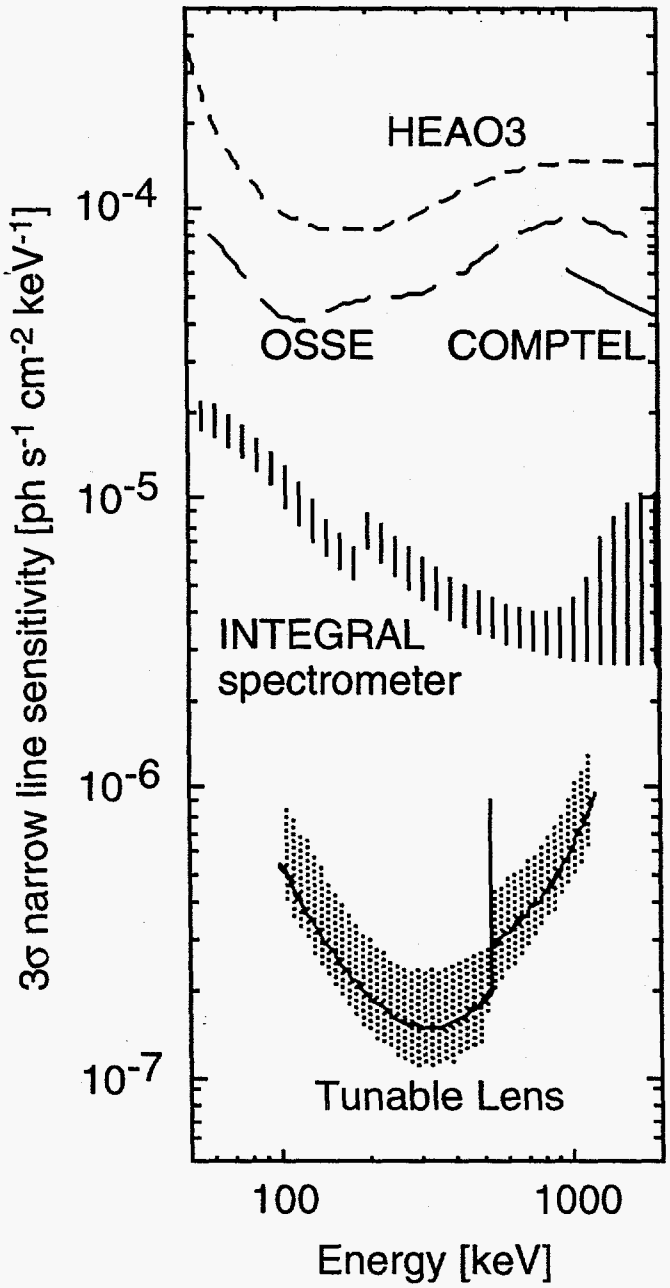

Figure 16 The estimated sensitivity of the presented instrument together with the sensitivities of past, present, and future telescopes. For a crystal lens telescope, the point source sensitivity depends on the diffraction efficiency of the lens, the full energy peak efficiency and the background of the detector.

7. APPLICATION TO ASTROPHYSICS EXPERIMENTS

A number of papers have been published that estimate the sensitivity of the crystal diffraction lens for seeing the emission of radioactive lines from astrophysical sources. The ideal situation would be to have a large lens mounted on a satellite where the pointing stability would be good and the focal length could be long. Both of these features are important. The good pointing stability would allow one to use crystals with small mosaic structure widths, which would enhance the efficiency of the diffraction process, and the long focal length would allow one to use a large lens and a lens that could be used for diffracting more energetic gamma rays. Figure 16 shows a comparison of the sensitivity of a crystal lens that is 100 cm in diameter with the present satellites in space, HEAO3, OSSE, and COMPTEL, and also with the predicted sensitivity of the very large INTEGRAL satellite that is planned for the near future.[10] The predicted improvement for this special application is quite impressive. The results depend on being able to field a lens of this size with a long focal length and with the line narrow enough in energy so that one can use crystals with relatively narrow mosaic structure widths. In this example, one used a mosaic structure width of 10 arc sec. This lens will have a field of 16 arc sec, thus good pointing is essential.

8. ACKNOWLEDGMENTS

This work was supported in part by the DOE contract No. W-31-109-ENG-38, by the *Region Midi-Pynenees* (Toulouse) and the French Space Agency (CNES).

9. REFERENCES

1. R. K. Smither, "New Method for Focusing X-Rays and Gamma-Rays," Rev. Sci. Instrum. 44, 131-141 (1982).

2. R. K. Smither, "New Method for Focusing and Imaging X-Rays and Gamma-Rays with Diffraction Crystals," Symposium on Future X-Ray Experiments, X-Rays in the 80's, GSFC, Oct. 1981, NASA Tech. Mem. No. 83848 (1981).

3. R. K. Smither, "Gamma-Ray Telescopes Using Variable-Metric Diffraction Crystals," 11th Texas Symposium on Relativistic Astrophysics, Austin, Texas, Dec. 1981, Annal. of New York Acad. Sci. 422, 384 (1983).

4. R. K. Smither and N. Lund, "A Bragg Crystal Flux Concentrator for Annihilation Radiation," 16th Inter. Cosmic Ray Conference, Banggalore, India, (1983). Published in the proceedings of the conference, supplement issue of AP.

5. R. K. Smither, "Crystal Diffraction Lenses for Imaging Gamma-Ray Telescope," 13th Texas Symposium on Relativistic Astrophysics, Chicago, IL, December 1986. Published as part of the proceedings as a book entitled *13th Texas Symposium on Relativistic Astrophysics,* ed. M.P. Ulmer, Northwestern Un., pp. 55-59, World Scientific Publishing Co., Singapore.

6. R. K. Smither, L. Greenwood and C. Roche, "Crystal Diffraction Telescope for Discrete Line Sources: Recent Experimental Results," GRO Science Workshop, Goddard Space Flight Center, April 1989, published as a NASA Report, "Gamma Ray Observatory Science Workshop", Goddard Space Flight Center, Greenbelt, Maryland, Editor, W. Neil Johnson.

7. Peter von Ballmoos and Robert K. Smither, "A Positron Annihilation Radiation Telescope Using Laue Diffraction in a Crystal Lens," International Gamma-Ray Astrophysics Laboratory INTEGRAL Workshop, Feb. 2-5 at Les Diablerets, Switzerland. AP supp., Vol. 92, 1994 June, 663.

8. R. K. Smither, P. v. Ballmoos, P. B. Fernandez, T. Graber, J. Naya, F. Albernhe, and G. Vedrenne, "Review of Crystal Diffraction and its Application to Focusing Energetic Gamma rays," Experimental Astronomy 6, 47-56 (1995).

9. J. E. Naya, R. K. Smither, P.v. Ballmoos, F. Albernhe, M. Faiz, P. B. Fernandez, T. Graber, and G. Vedrenne, "Experimental Results Obtained with the Positron Annihilation-Radiation Telescope of the Toulouse-Argonne Collaboration," Paper presented at the Symposium on Imaging in High Energy Astronomy, Anacapri, Italy, Sept. 26-30, 1994. Published as part of the proceedings: L Bassani and G. di Cocco (eds), *Imaging in High Energy Astronomy.*

10. P.v. Ballmoos, R. K. Smither, J. E. Naya, F. Albernhe, M. Faiz, P. B. Fernandez, T. Graber, and G. Vedrenne "A Tunable Crystal Diffraction Telescope for the Energy Range of Nuclear Transitions," Paper presented at the Symposium on Imaging in High Energy Astronomy, Anacapri, Italy, Sept. 26-30, 1994. Published as part of the proceedings: L Bassani and G. di Cocco (eds), *Imaging in High Energy Astronomy.*

11. R. K. Smither and P.v. Ballmoos, "Gamma-Ray Line Astrophysics with a Crystal Diffraction Lens System," Paper presented at the 17th Texas Symposium for Relativistic Astrophysics, Munich, Dec. 12-17, 1994. Published by the New York Academy of Sciences as part of the proceedings (1996).

DISCLAIMER